

Thermal conductivity of isotopically pure and Ge-doped Si epitaxial layers from 300 to 550 K

David G. Cahill* and Fumiya Watanabe

Department of Materials Science and Engineering, and Frederick Seitz Materials Research Laboratory, University of Illinois, Urbana, Illinois 61801, USA

(Received 29 September 2004; published 17 December 2004)

The thermal conductivity of epitaxial layers of Si is measured in the temperature range $300 < T < 550$ K using time-domain thermoreflectance. The analysis of the thermoreflectance data uses the ratio of the in-phase and out-of-phase signals of the lock-in amplifier to achieve a precision of $\pm 5\%$. Comparisons are made between epitaxial layers of isotopically pure ^{28}Si , Si with a natural isotope abundance, and Ge-doped Si. At 297 K, the thermal conductivity of ^{28}Si epitaxial films is $16 \pm 5\%$ larger than the thermal conductivity of natural Si. The thermal resistance created by mass-disorder scattering of phonons is in good agreement with theory for natural Si and for Ge-doped Si with a Ge concentration of $1.4 \times 10^{19} \text{ cm}^{-3}$.

DOI: 10.1103/PhysRevB.70.235322

PACS number(s): 66.70.+f

Most natural crystals contain a mixture of isotopes that disrupts the perfect periodicity of the lattice; isotope mixtures reduce the lifetimes of high-frequency phonons and the thermal conductivity. The effective strength of phonon scattering by mass disorder is increased by anharmonic interactions between the phonons. For example, the so-called “normal (N) processes” conserve crystal momentum and therefore do not contribute directly to the thermal resistance.¹ But high-frequency phonons produced by N processes are strongly scattered by mass disorder and this combination of N processes and mass-disorder scattering can produce a significant contribution to the thermal resistivity of a crystal. Therefore, an isotopically pure crystal is expected to have an enhanced thermal conductivity, and isotopically pure diamond does indeed display a large enhancement, nearly 40% at room temperature.² Diamond, however, is an unusual crystal with an extremely high Debye temperature and low anharmonicity. Thorough studies of ^6LiF - ^7LiF mixtures show that isotope purity has little effect on the thermal conductivity at $T > 70$ K.^{3,4}

The thermal conductivity of isotopically pure ^{28}Si has been controversial. The first study of epitaxial layers of ^{28}Si reported that the thermal conductivity near room temperature was enhanced by 60% relative to natural Si;⁵ subsequent calculations⁶ found acceptable agreement between theory and experiment. Measurements of a single crystal⁷ of ^{28}Si were initially thought to confirm the original experiments but the authors of Ref. 7 later retracted that conclusion and now report a change in conductivity of only $\approx 10\%$ at room temperature.⁸ Another study of ^{28}Si single crystals⁹ obtained a similar value, $\approx 7\%$. Other theories^{10,11} predict a $\approx 12\%$ enhancement. Recently, a second experimental study of epitaxial layers reported a 55% enhancement.¹²

These divergent results—and the conjecture that ^{28}Si will facilitate thermal management of microelectronics—motivated us to reexamine the thermal conductivity of epitaxial layers of ^{28}Si and extend the data to elevated temperatures, $300 < T < 550$ K. (High-speed, high-density Si devices typically operate at temperatures $350 < T < 400$ K.) We compare our new data for ^{28}Si to measurements of natural Si and to Ge-doped layers. The difference in conductivity between epitaxial layers of ^{28}Si and natural Si, $16 \pm 5\%$, is slightly

larger than what was found in prior experiments on single crystals^{8,9} but a factor of 3–4 smaller than previous studies of epitaxial layers.^{5,12} Data for lightly Ge-doped layers are in good agreement with a linear extrapolation of the theoretical predictions¹¹ to higher levels of mass disorder.

Isotopically pure ^{28}Si epitaxial layers of two thicknesses, 5 and 92 μm , were supplied by Dr. S. Burden of Isonics Corp. The isotope purity is $>99.9\%$. The 5 μm layer was grown from a silane precursor and was not intentionally doped; the 92 μm layer was grown from trichlorosilane and was *B* doped to $\approx 10^{16} \text{ cm}^{-3}$. The exact thickness of the layers is not important because these thicknesses are much larger than the thermal penetration depth of the experiment, $\sqrt{D/(2\pi f)} = 1.3 \mu\text{m}$ at 297 K. A standard electronic-grade “epi” wafer with a natural abundance of the Si isotopes was used for comparison. The thickness of this epitaxial layer is $\approx 15 \mu\text{m}$ and the *p*-type resistivity is $\approx 10 \Omega \text{ cm}$. Two epitaxial layers of Ge-doped Si were grown at the Seitz Materials Research Laboratory using disilane and digermane precursors at a growth temperature of 973 K; the thickness of these layers is 1.3 μm . The Ge content was measured to an accuracy of $\pm 10\%$ by secondary ion mass spectrometry (SIMS); the secondary ion yields were calibrated using a sample with a much higher Ge concentration (1.4% Ge) where the Ge concentration was measured using Rutherford backscattering spectrometry.

The five test samples were coated with ≈ 100 nm of Al by magnetron sputter deposition with the substrates at room temperature. An accurate thickness of the Al layers is crucial for the data analysis; the thickness of the Al film is measured simultaneously with the thermal measurements using picosecond acoustics and a longitudinal speed of sound $v_l = 6.42 \text{ nm ps}^{-1}$. Sample temperatures are measured by a miniature Pt resistance thermometer that is attached to the front side of the sample with Ag paint.

Figure 1 shows typical thermoreflectance data and fit to the thermal model.¹³ In principle, the thermal model needed to analyze the experiments contains seven parameters: the thickness h , specific heat C , and thermal conductivity Λ of the Al film; the diameter of the laser spot; the thermal conductance of the Al/Si interface and the thermal conductivity and heat capacity of the Si sample. But because the thermal

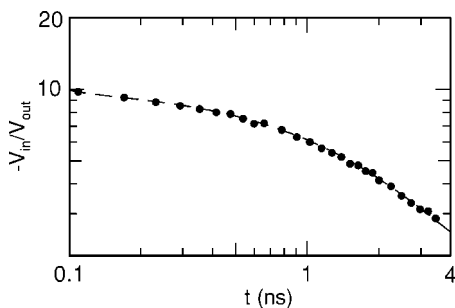


FIG. 1. Time-domain thermorefectance data acquired at room temperature for a Al/Si sample. The ratio of the in-phase to out-of-phase signals at the 9.8 MHz modulation frequency is plotted as a function of the delay time t . The dashed-line is the best fit to the thermal model with the thermal conductivity Λ of ^{28}Si and the Al/Si interface thermal conductance G as the free parameters; this fit gives $\Lambda=1.64 \text{ W m}^{-1}\text{K}^{-1}$ and $G=185 \text{ MW m}^{-2}\text{K}^{-1}$.

conductivity of the Al film is high and the film thickness is small, Λ_{Al} is relatively unimportant but the fit is sensitive to the total heat capacity per unit area of the Al film, $h_{\text{Al}}C_{\text{Al}}$. The heat capacities of Al and Si are tabulated in Refs. 14 and 15, respectively. (We estimate that the difference in the heat capacity per unit volume of ^{28}Si and natural Si is less than 0.2% at room temperature.) We make a small correction to the heat capacity of the Al film by adding the heat capacity of a 2 nm layer of Al_2O_3 . Since the thermal penetration depth is small compared to the $1/e^2$ radius of the laser spot w_0 , heat flow in the experiment is predominately one dimensional but radial heat flow in cylindrical coordinates is included in the thermal model; thus, the measured size of the laser spot $w_0 \approx 8 \mu\text{m}$ is a parameter in the analysis. Two free parameters, Λ , the thermal conductivity of the Si epitaxial layer, and G , the thermal conductance of the Al/Si interface, are varied to fit the data.

In Fig. 2, we plot the so-called ‘‘sensitivity parameters’’ S_α for the experimental data of Fig. 1.

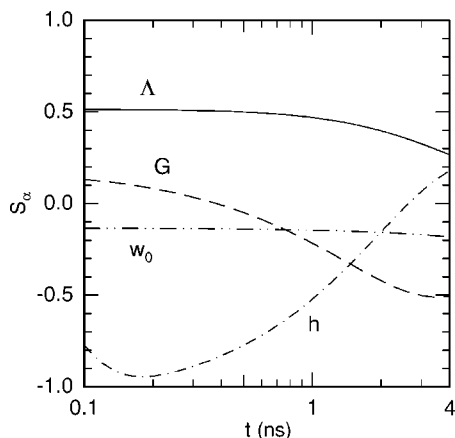


FIG. 2. Sensitivity coefficients S_α for the experiment shown in Fig. 1; see Eq. (1) for the definition of S_α . The curves are labeled by the parameters in the thermal model: Λ is the thermal conductivity of Si epitaxial layer, G the thermal conductance of the Al/Si interface, h the thickness of the Al film, and w_0 the $1/e^2$ radius of the laser spot.

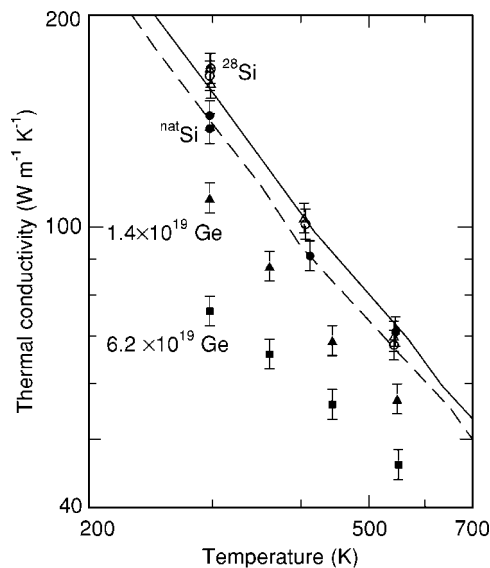


FIG. 3. Thermal conductivity of epitaxial Si layers: natural Si (solid circles); isotopically pure ^{28}Si 92 μm thick (open circles); ^{28}Si 5 μm thick (open triangles); and Ge-doped Si (solid triangles and solid squares). Data for the two Ge-doped layers are labeled by the Ge concentration in units of cm^{-3} . The solid and dashed lines are data for natural Si from Refs. 17 and 18, respectively.

$$S_\alpha = \frac{d \ln(-V_{\text{in}}/V_{\text{out}})}{d \ln \alpha}, \quad (1)$$

where α can be any one of the seven parameters in the thermal model.¹³ As we have noted previously¹⁶, $V_{\text{in}}/V_{\text{out}}$ scales with the square root of Λ and is relatively independent of G for short-to-intermediate times, $0.1 < t < 1 \text{ ns}$; and G can be determined accurately by the stronger dependence of $V_{\text{in}}/V_{\text{out}}$ on G at long times, $t > 2 \text{ ns}$. Uncertainties in the Al film thickness are important in setting the limits to the precision of our measurements; we estimate those uncertainties as $\pm 2\%$, which propagate into errors in Λ of $\pm 4\%$. The precision is also reduced by laser noise and systematic errors in the measurement of the out-of-phase signal V_{out} . Our experience with many measurements of Si, MgO, Al_2O_3 , SiO_2 , and metals¹⁶ lead us to conclude that the overall precision is $\approx \pm 5\%$. (Uncertainties in the heat capacity per unit volume of the Al film and the Si sample and uncertainties in the laser spot size reduce the accuracy of our measurements but not the precision.)

The thermal conductivity data as a function of temperature are summarized in Fig. 3. Data for natural Si are in good agreement with accepted values;^{18,19} the thermal conductivity of ^{28}Si is noticeably larger at room temperature and 400 K but the differences are not apparent at 550 K. The averages of the measurements for natural Si give $\Lambda=142, 91$, and $70 \text{ W m}^{-1}\text{K}^{-1}$ at 297, 412, and 545 K, respectively; for ^{28}Si , the averages are $\Lambda=165, 102$, and $69 \text{ W m}^{-1}\text{K}^{-1}$ at 297, 405, and 542 K, respectively. We conclude from these data that the use of isotopically pure Si substrates will have only a modest impact on the thermal management of Si microelectronic devices operating at temperatures near 370 K.

Since the changes in conductivity are not large compared

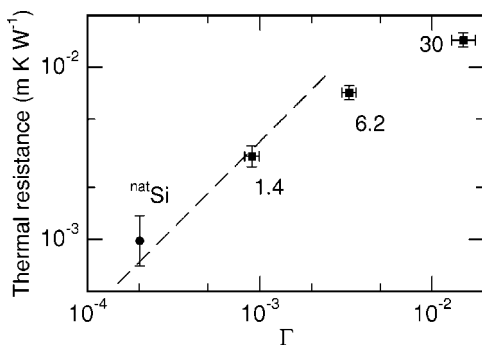


FIG. 4. Thermal resistance generated by mass-disorder phonon scattering in Si at 297 K. The data points are for natural Si (filled circle), and Si doped with Ge (filled squares). The points for Ge-doped Si are labeled by the Ge concentration in units of 10^{19} cm^{-3} ; the data point for $30 \times 10^{19} \text{ cm}^{-3}$ is for a SiGe single crystal measured by Yonenaga *et al.* (see Ref. 20). Γ is a dimensionless parameter that describes the strength of the phonon scattering [see Eq. (2)].

to the precision of the measurements, we have also investigated Ge-doped layers to increase the strength of the mass-disorder scattering; these data are included in Fig. 3 and show that a Ge concentration of $6.2 \times 10^{19} \text{ cm}^{-3}$ is sufficient to reduce the thermal conductivity of Si by nearly a factor of two.

In the limit of weak scattering, phonon scattering by mass disorder is expected to scale with the concentration and the square of the mass difference.²¹ The strength of scattering can be characterized by the following dimensionless parameter^{11,21,22}

$$\Gamma = \sum_i c_i \left(\frac{m_i - \bar{m}}{\bar{m}} \right)^2, \quad (2)$$

where c_i is the fractional concentration of the i th species, m_i is the atomic mass of the i th species, and \bar{m} is the average atomic mass. For natural Si, $\Gamma = 2.0 \times 10^{-4}$.

In Fig. 4, we plot the thermal resistance created by the mass-disorder scattering using the measured thermal conductivity of ^{28}Si as the baseline. A linear extrapolation of the theoretical prediction¹¹ is shown as a dashed line. At the highest level of Γ , the thermal resistance falls below this linear extrapolation; the thermal resistance is expected to follow a $\Gamma^{1/2}$ dependence when the thermal resistance created by mass-disorder scattering exceeds the intrinsic thermal resistance.²¹ The good agreement between the weak-scattering limit of the theory, data for phonon scattering in natural Si, and data for Si with $1.4 \times 10^{19} \text{ cm}^{-3}$ Ge supports our conclusion that the natural isotope mixtures in Si produce only a small increase in the thermal resistance near room temperature.

We thank Professor A. Rockett for contributing his time and expertise in SIMS analysis of the Ge-doped layers, and Dr. D. Morelli for bringing this problem to our attention. This work was supported by the U.S. Department of Energy, Division of Materials Sciences under Grant No. DEFG02-91ER45439, through the Frederick Seitz Materials Research Laboratory (MRL) at the University of Illinois at Urbana-Champaign. Sample characterization used the facilities of the Center for Microanalysis of Materials, which is partially supported by the U.S. Department of Energy under Grant No. DEFG02-91ER45439; and the Laser Facility of the MRL.

*Electronic address: d-cahill@uiuc.edu

¹D. G. Cahill and R. O. Pohl, *Annu. Rev. Phys. Chem.* **39**, 93 (1988).

²L. Wei, P. K. Kuo, R. L. Thomas, T. R. Anthony, and W. F. Banholzer, *Phys. Rev. Lett.* **70**, 3764 (1993).

³R. Berman and J. C. F. Brock, *Proc. R. Soc. London, Ser. A* **289**, 46 (1965).

⁴P. D. Thacher, *Phys. Rev.* **156**, 975 (1967).

⁵W. S. Capinski, H. J. Maris, E. Bauser, I. Silier, M. Asen-Palmer, T. Ruf, M. Cardona, and E. Gmelin, *Appl. Phys. Lett.* **71**, 2109 (1997).

⁶W. S. Capinski, H. J. Maris, and S. Tamura, *Phys. Rev. B* **59**, 10 105 (1999).

⁷T. Ruf, R. W. Henn, M. Asen-Palmer, E. Gmelin, M. Cardona, H.-J. Pohl, G. G. Devyatych, and P. G. Sennikov, *Solid State Commun.* **115**, 243 (2000).

⁸T. Ruf, R. W. Henn, M. Asen-Palmer, E. Gmelin, M. Cardona, H.-J. Pohl, G. G. Devyatych, and P. G. Sennikov, *Solid State Commun.* **127**, 257 (2003).

⁹A. V. Gusev, A. M. Gibin, O. N. Morozkin, V. A. Gavva, and A. V. Mitin, *Inorg. Mater.* **38**, 1305 (2002).

¹⁰A. P. Zhernov, *J. Exp. Theor. Phys.* **93**, 1074 (2001).

¹¹D. T. Morelli, J. P. Heremans, and G. A. Slack, *Phys. Rev. B* **66**,

195304 (2002).

¹²P. L. Komarov, M. G. Burzo, G. Kaytaz, and P. E. Raad, *Microelectron. J.* **34**, 1115 (2003).

¹³R. M. Costescu, M. A. Wall, and D. G. Cahill, *Phys. Rev. B* **67**, 054302 (2003).

¹⁴A. J. Leadbetter, *J. Phys. C* **1**, 1481 (1968).

¹⁵H. R. Shanks, P. D. Maycock, P. H. Siddles, and G. C. Danielson, *Phys. Rev.* **130**, 1743 (1963).

¹⁶S. Huxtable, D. G. Cahill, V. Fauconnier, J. O. White, and J.-C. Zhao, *Nat. Mater.* **3**, 298 (2004).

¹⁷C. J. Glassbrenner and G. A. Slack, *Phys. Rev.* **134**, A1058 (1964).

¹⁸W. Fulkerson, J. P. Moore, R. K. Williams, R. S. Graves, and D. L. McElroy, *Phys. Rev.* **167**, 765 (1968).

¹⁹D. S. Beers, G. P. Cody, and B. Abeles, in *Proceedings of the International Conference on the Physics of Semiconductors, Exeter* (Institute of Physics, London, 1962), pp. 41–48.

²⁰I. Yonenaga, T. Akashi, and T. Goto, *J. Phys. Chem. Solids* **62**, 1313 (2001).

²¹B. Abeles, *Phys. Rev.* **131**, 1906 (1963).

²²P. G. Klemens, *Proc. Phys. Soc., London, Sect. A* **68**, 1113 (1955).